Supporting Information

Temperature-dependent structural transition following X-ray-induced metal center reduction in oxidized cytochrome *c* oxidase

Izumi Ishigami, Silvia Russi, Aina Cohen, Syun-Ru Yeh, and Denis L. Rousseau

The material includes:

1. Supporting text
2. Figures S1-S4
3. Tables S1-S2

Supporting Text.

Assignment of optical absorption bands. In the optical absorption spectra of bC*c*O crystals in the oxidized and reduced states shown in Fig. 2A, the contributions from each of the hemes are assigned based on the spectral analysis reported by Vanneste (34). For the reduced spectrum, the Soret band at 440 nm is attributed to hemes a^{2+} and a_3^{2+}, while the sharp visible band at 600 nm band is mostly assigned to heme a^{2+}, with a minor contribution from heme a_3^{2+} (~4 times weaker than that of heme a^{2+}). For the oxidized spectrum, the major Soret band at 426 nm is attributed to heme a^{3+}, while the shoulder at ~ 414 nm, with ~2/3 the intensity of the major band, is assigned to heme a_3^{3+}. It should be noted that the apparent Soret maximum of the oxidized enzyme appears at ~424 or ~418 nm for “fast” or “slow” enzyme, respectively, depending on the enzyme preparation (45,46). In our solution spectra (Fig. 2B), the Soret band of the resting oxidized enzyme is centered at 424 nm, indicating that our enzyme is in the fast form.

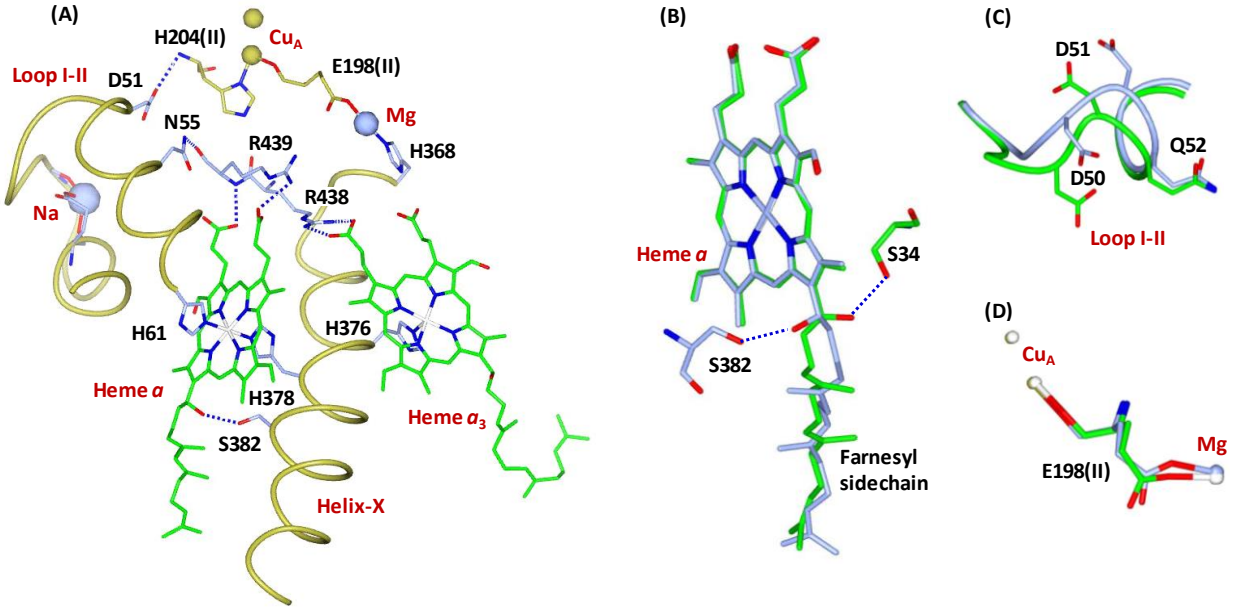

Fig. S1. H-bonding network linking Cu_A to heme *a* and heme a_3 (A) and the major redox-dependent structural differences between the fully oxidized O structure and the fully reduced R structure (B-D). The fully oxidized **O** and reduced **R** structures are based on PDB 7TIE and 7THU, respectively. The structure in (A) is taken from the fully oxidized **O** structure. The dashed lines indicate H-bonds within a bond distance <3 Å. Helix X contains the axial ligands to heme *a* and heme a_3 (H378 and 376, respectively). It is linked to Cu_A *via* the Mg ion and its ligands, H368, and E198 (II). Cu_A is connected to Loop I-II (linking Helix I to Helix II) *via* an H-bond between its ligand, H204 (II), and D51 in the loop. Loop I-II is subsequently connected to heme *a* and heme a_3 *via* a H-bonding network involving N55, R439/R438, and the propionate groups of the two heme moieties. The Na ion sitting at one edge of the Loop I-II plays a role in stabilizing the loop structure. All the structural elements are from subunit-I, except H204(II) and E198(II) are from subunit-II as indicated in the parenthesis. Owing to these interlaced interactions, the changes in the redox and/or ligation states of the metal centers associated with the O_2 reduction reaction occurring in the BNC are transmitted to the protein matrix surrounding them, thereby driving proton translocation. In (B-D), the oxidized (**O**) and reduced (**R**) structures are depicted in blue and green, respectively. The major redox-dependent structural differences between the **O** and **R** species involving heme *a*, Loop I-II and the CuA-198(II)-Mg moiety are shown in (B), (C) and (D), respectively. The change in the oxidation state of heme *a* induces 120° rotation of its farnesyl sidechain and its H-bonding with S382 or S34, while the change in the oxidation state of Cu_A likely leads to the conformational change in Loop I-II (C), as well as that of E198(II) bridging Cu_A to the Mg (D).

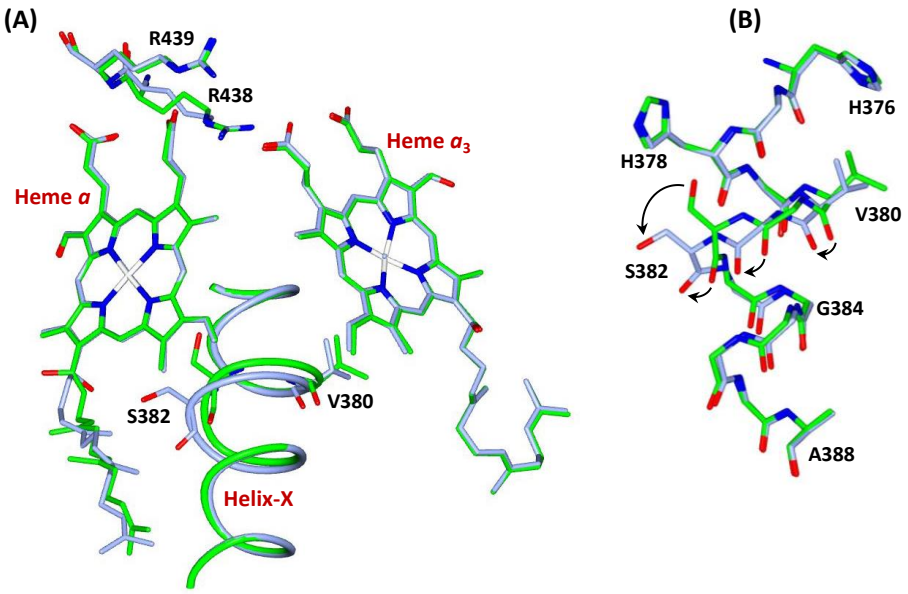

Fig. S2. Comparison of the Helix X and R438 structures in the reduced ligand-free R state (green) *versus* the oxidized ligand-bound O state (blue). (A) Helix X adopts a normal α-helical structure in the ligand-free **R** state, but when a ligand is coordinated to the heme a_3 iron atom the helical structure in the [380-385] region is disrupted leading to a bulge in the polypeptide backbone and reorientation of the S382 sidechain. The structural changes are associated with the rotation of the R438 sidechain. (B) The changes in Helix-X structure resulting from ligand binding to heme a_3 is highlighted by the black arrows. It is important to note that the same structural rearrangements described above are observed upon CO binding to the **R** species (see PDB 5W97 *versus* PDB 5WAU), indicating that they are sensitive to ligand binding to heme a_3, regardless of the metal oxidation states (21). The **O** and **R** structures are based on PDB 7TIE and 7THU, respectively.

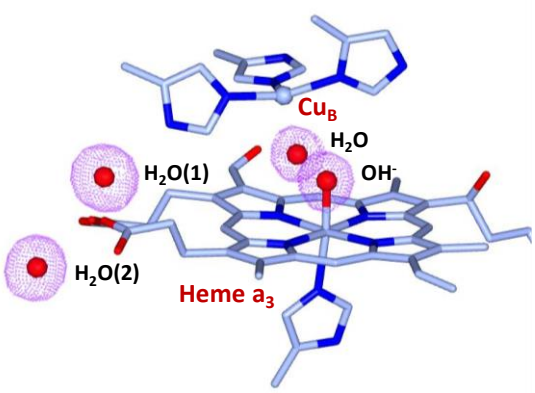

Fig. S3. **Polder maps of the OH^- and H_2O ligands in the BNC in the O* state of bC*c*O and the two nearby H_2O molecules labelled (1) and (2) used as intensity references.** The polder map for each ligand was calculated separately. They were contoured at 8.0 σ. The electron densities of the reference water molecules were averaged and used as a reference to calculate the ligand occupancies listed in Table S2. The same method was used to calculate the ligand occupancies in **R*** (not shown).

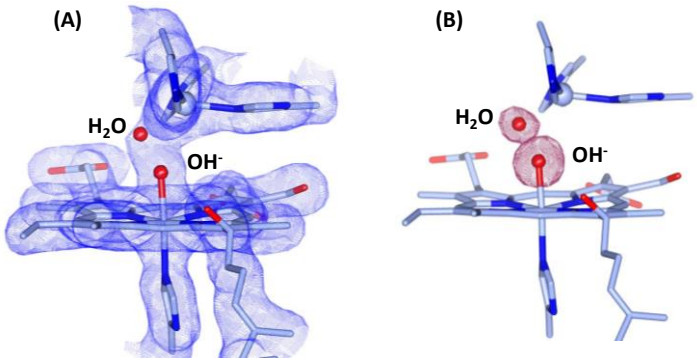

Fig. S4. The $2F_O$-F_C map (A) and polder maps (B) of the BNC in the comparable oxidized bC*c*O structure obtained at APS (PDB code 7TIE). The binuclear center was modeled with a hydroxide ion that is coordinated to heme a_3 and a water molecule that is 2.34 Å away from Cu_B. The two oxygen are separated by a distance of 1.91 Å. The polder map for each ligand was calculated separately. The occupancies of the hydroxide ion and the water molecule are estimated to be 96% and 63%, respectively, based on the method described in Fig. S3. The two reference water molecules are not shown. The $2F_O$-F_C map and the polder maps were contoured at 1.5 and 8.0 σ, respectively.

Table S1. Crystallographic data collection and refinement statistics. The **O*** and **R*** structural data were obtained before and after annealing, respectively, on beam line BL9-2 at SSRL. The reduced (**R**) structure and a comparable **O*** structure were obtained on beam line 31-ID-D at the APS.

	Oxidized (**O***) (Before anneal)	Reduced (**R***) (After Anneal)	Oxidized (**O***) (Reference set)	Reduced (**R**) (Reference set)
PDB Accession code	7TIH	7TII	7TIE	7THU
Data Collection				
Source	SSRL BL9-2	SSRL BL9-2	APS 31-ID-D	APS 31-ID-D
Wavelength (Å)	0.9795	0.9795	0.9793	0.9793
Beam size (μ)	100 x 60	100 x 60	110 x 80	110 x 80
Space group	$P2_12_12_1$	$P2_12_12_1$	$P2_12_12_1$	$P2_12_12_1$
Dimensions: a, b, c (Å)	178.04, 182.7, 205.85	178.04, 182.63, 205.45	178.12, 182.41, 208.55	178.18, 182.28, 208.68
Dimensions: α, β, γ (°)	90,90,90	90,90,90	90,90,90	90,90,90
Resolution	40-2.35	40-2.45	40-1.90	40-1.93
I/σI	6.7 (1.0)	6.9 (0.9)	7.8 (1.0)	12.6 (1.0)
$CC_{1/2}$	0.993 (0.456)	0.993 (0.402)	0.996 (0.442)	0.999 (0.416)
Multiplicity	3.4 (3.4)	6.9 (7.0)	6.9 (6.8)	6.8 (6.9)
Refinement				
Resolution (Å)	39.34-2.35	39.30-2.45	39.99-1.90	40-1.93
Completeness (%)	99.85 (99.85)	99.85 (99.90)	99.83 (99.77)	99.13 (99.50)
Unique reflections	263,771	232,416	501,266	475,873
R_{work}/R_{free}	0.1930/0.2351	0.2063/0.2530	0.1846/0.2152	0.1836/0.2125
Number of atoms	32,721	32,401	32,913	32,695
Mean B factor ($Å^2$)	45.60	46.83	43.50	46.82
RMS Deviations				
Bond lengths (Å)	0.009	0.008	0.015	0.015
Bond angles (°)	1.618	1.622	1.678	1.688

Table S2. Electron densities and the estimated occupancies of the oxygen ligands in the BNC of bC*c*O in the O* and R* states. The ligand occupancies were calculated with respect to two nearby water molecules (indicated as "Reference*") based on polder map analysis described in Fig. S3.

	O*		**R***	
	$e^-/Å^3$	Occupancy	$e^-/Å^3$	Occupancy
Reference*	0.91	100%	0.79	100%
OH^-	0.78	86%	0.54	63%
H_2O	0.73	80%	0.30	35%